

Quantum phase transition between disordered and ordered states in the spin- $\frac{1}{2}$ kagome lattice antiferromagnet $(\text{Rb}_{1-x}\text{Cs}_x)_2\text{Cu}_3\text{SnF}_{12}$

Kazuya Katayama,* Nobuyuki Kurita,† and Hidekazu Tanaka‡
*Department of Physics, Tokyo Institute of Technology,
Oh-okayama, Meguro-ku, Tokyo 152-8551, Japan*

(Dated: July 24, 2018)

We have systematically investigated the variation of the exchange parameters and the ground state in the $S = 1/2$ kagome-lattice antiferromagnet $(\text{Rb}_{1-x}\text{Cs}_x)_2\text{Cu}_3\text{SnF}_{12}$, via magnetic measurements using single crystals. One of the parent compounds, $\text{Rb}_2\text{Cu}_3\text{SnF}_{12}$, which has a distorted kagome lattice accompanied by four sorts of nearest-neighbor exchange interaction, has a disordered ground state described by a pinwheel valence-bond-solid state. The other parent compound, $\text{Cs}_2\text{Cu}_3\text{SnF}_{12}$, which has a uniform kagome lattice at room temperature, has an ordered ground state with the $q = 0$ spin structure. The analysis of magnetic susceptibilities shows that with increasing cesium concentration x , the exchange parameters increase with the tendency to be uniform. It was found that the ground state is disordered for $x < 0.53$ and ordered for $x > 0.53$. The pseudogap observed for $x < 0.53$ and the Néel temperature for $x > 0.53$ approach zero at $x_c \simeq 0.53$. This is indicative of the occurrence of a quantum phase transition at x_c .

PACS numbers: 75.10.Jm, 75.10.Kt, 75.40.Cx

I. INTRODUCTION

Geometrically frustrated quantum antiferromagnets, a research frontier in condensed matter physics, have been attracting growing attention owing to the potential realization of exotic ground states such as the spin liquid state.¹ One of the simplest and most intriguing frustrated magnets is a Heisenberg antiferromagnet on the kagome lattice (KLAF) composed of corner-sharing triangles. For the classical Heisenberg KLAF with the nearest-neighbor exchange interaction, the ground state is infinitely degenerate owing to the local flexibility of the configuration of the 120° spin structure characteristic of the kagome lattice. In the case of a non-classical Heisenberg spin with a large spin quantum number, it has been predicted that the so-called $\sqrt{3} \times \sqrt{3}$ structure is stabilized by the order-by-disorder mechanism.^{2,3} The most intriguing case is the spin- $\frac{1}{2}$ case, where a noteworthy synergistic effect of the geometric frustrations, the local flexibility, and the quantum fluctuations is expected. A long theoretical debate has reached the consensus that the quantum-disordered state is more stable than any ordered state. However, the nature of the ground state has not been theoretically elucidated. Recent theory suggests the nonmagnetic ground states, such as the valence-bond-solid⁴⁻⁸ and quantum spin-liquid states,⁹⁻¹¹ which are described by a static array of singlet dimers and the superposition of various configurations composed of singlet dimers, respectively. The nature of low-energy excitations also remains unresolved. The presence of a gap for the triplet excitation is still controversial.¹²⁻¹⁶

On the experimental side, considerable effort has been made to search for materials that closely approximate the spin- $\frac{1}{2}$ Heisenberg KLAF.¹⁷⁻²⁴ However, the materials investigated, many of which are natural minerals, have individual problems such as spatial anisotropy of

the exchange network^{18,25}, exchange disorder due to ion substitution²⁶ and lattice distortion due to a structural phase transition.²⁷ For these reasons, there has been little clear experimental evidence demonstrating the nature of the ground state and the excitations for the spin- $\frac{1}{2}$ Heisenberg KLAF.

The cupric fluoride kagome family, $A_2\text{Cu}_3\text{SnF}_{12}$ ($A = \text{Rb}$ and Cs), which has a trigonal structure, is promising for the comprehensive study of spin- $\frac{1}{2}$ KLAFs.^{28,29} Figures 1(a) and (b) show the crystal structures of $\text{Rb}_2\text{Cu}_3\text{SnF}_{12}$ and $\text{Cs}_2\text{Cu}_3\text{SnF}_{12}$ viewed along the c axis, respectively. CuF_6 octahedra are linked by sharing their corners in the crystallographic ab plane. Magnetic Cu^{2+} ions with spin- $\frac{1}{2}$ form a kagome lattice in the ab plane. The octahedra are elongated along the principal axes, which is approximately parallel to the c axis owing to the Jahn-Teller effect. Hence, the hole orbitals $d(x^2 - y^2)$ of Cu^{2+} are spread in the kagome layer. This leads to a strong superexchange interaction in the kagome layer and a negligible superexchange interaction between layers.

At room temperature, $\text{Rb}_2\text{Cu}_3\text{SnF}_{12}$ has a $2a \times 2a$ enlarged chemical unit cell in the ab plane, as shown in Fig. 1(a); thus, the kagome lattice in $\text{Rb}_2\text{Cu}_3\text{SnF}_{12}$ is not uniform.²⁸ There are four sorts of nearest-neighbor exchange interactions as depicted in Fig. 1(c).²⁸ $\text{Cs}_2\text{Cu}_3\text{SnF}_{12}$ has a uniform kagome lattice at room temperature.²⁹ As the temperature decreases, $\text{Cs}_2\text{Cu}_3\text{SnF}_{12}$ undergoes a structural phase transition from the trigonal structure to the monoclinic structure at $T_t = 184$ K,³⁰ which is closely related to the trigonal structure with a $2a \times 2a$ enlarged unit cell.^{29,31}

Since high-purity and sizable single crystals are obtainable, the magnetic properties of these two compounds have been probed in detail by magnetic, neutron scattering and NMR measurements.³¹⁻³⁴ The magnetic ground

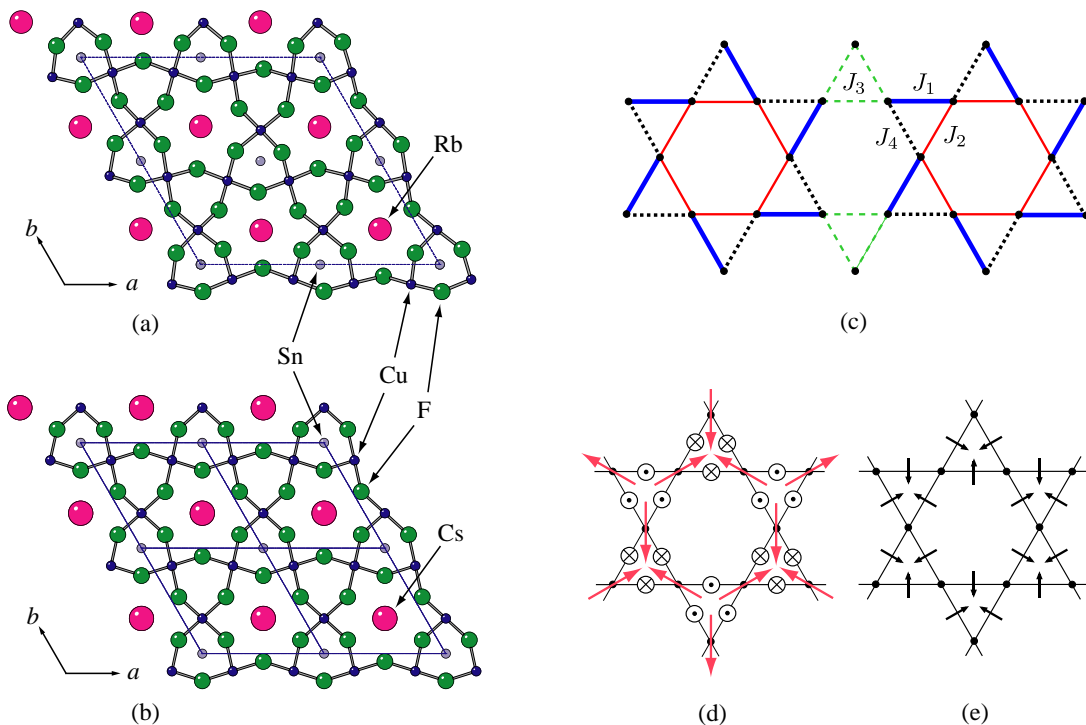


FIG. 1: Crystal structures of (a) $\text{Rb}_2\text{Cu}_3\text{SnF}_{12}$ and (b) $\text{Cs}_2\text{Cu}_3\text{SnF}_{12}$ viewed along the c axis, where F^- ions located outside the kagome layer are omitted. Thin dotted lines denote the chemical unit cells. (c) Configuration of the exchange interactions J_i ($i=1-4$) for $\text{Rb}_2\text{Cu}_3\text{SnF}_{12}$. Arrangement of the \mathbf{D} vectors of the DM interaction: (d) c -axis component D^{\parallel} and (e) c -plane component D^{\perp} . The circled dots and circled crosses in (d) and the arrows in (e) represent the local positive directions of the parallel and perpendicular components D^{\parallel} and D^{\perp} , respectively. The large arrows in (d) indicate the $q=0$ structure stabilized by the DM interaction.

state of $\text{Rb}_2\text{Cu}_3\text{SnF}_{12}$ is a spin singlet with an excitation gap Δ/k_{B} of 27 K.^{28,32-34} Neutron inelastic scattering experiments revealed that the ground state is the pin-wheel valence-bond-solid (VBS) state, in which singlet dimers are situated on the strongest exchange interaction J_1 shown in Fig. 1(c).^{32,33,35,36} The gapped ground state in $\text{Rb}_2\text{Cu}_3\text{SnF}_{12}$ arises from the inequivalence of the exchange interactions, i.e., $J_1/k_{\text{B}} = 216$ K, $J_2 = 0.95J_1$, $J_3 = 0.85J_1$ and $J_4 = 0.55J_1$.³²

On the other hand, $\text{Cs}_2\text{Cu}_3\text{SnF}_{12}$ exhibits a magnetic ordering at $T_{\text{N}} = 20.0$ K.²⁹ In the ordered phase, the so-called $q=0$ spin structure is realized.³¹ The effect of the antisymmetric Dzyaloshinsky-Moriya (DM) type interaction on the ground state was investigated numerically by Cépas *et al.*,³⁷ who assumed the same configuration of the \mathbf{D} vector as that in $\text{Cs}_2\text{Cu}_3\text{SnF}_{12}$ [Fig. 1(d)]. They demonstrated that with increasing longitudinal component D^{\parallel} , the disordered state changes at $(D^{\parallel}/J)_{\text{c}} \approx 0.1$ to the ordered state with the $q=0$ structure. The magnitude of the \mathbf{D} vector in $\text{A}_2\text{Cu}_3\text{SnF}_{12}$ was evaluated to be $D^{\parallel}/J \simeq 1/4$ from the analyses of the dispersion relations.^{31,32} Thus, the magnetic ordering observed in $\text{Cs}_2\text{Cu}_3\text{SnF}_{12}$ can be attributed to the large DM interaction. Although the ground state of $\text{Cs}_2\text{Cu}_3\text{SnF}_{12}$ is ordered, a noteworthy quantum many-body effect on the

spin wave excitations was observed.³¹ The excitation energies are markedly renormalized downward with respect to the linear spin-wave result in contrast to the conventional quantum renormalization, in which the excitation energies are renormalized upward.³⁸⁻⁴²

In $\text{Rb}_2\text{Cu}_3\text{SnF}_{12}$, the lowest excitation is located at the Γ point, although the lowest excitation is expected to be located at the K point within the Heisenberg type exchange interaction. This is because the large DM interaction splits the triply degenerate triplet excitations into two levels, $S^z = 0$ and $S^z = \pm 1$ branches, and the energy of the $S^z = \pm 1$ branch is minimized at the Γ point with increasing magnitude of D^{\parallel} .^{32,43} If the inequivalence of the exchange interactions becomes small, it is expected that the gap at the Γ point will decrease and a transition from the singlet ground state to the ordered ground state will occur. The exchange interactions in $\text{Cs}_2\text{Cu}_3\text{SnF}_{12}$ are similar to those in the uniform case.³¹ Thus, we can expect a quantum phase transition in $(\text{Rb}_{1-x}\text{Cs}_x)_2\text{Cu}_3\text{SnF}_{12}$ upon varying the cesium concentration x . This motivated us to investigate the magnetic properties of $(\text{Rb}_{1-x}\text{Cs}_x)_2\text{Cu}_3\text{SnF}_{12}$.

In this paper, we present the results of magnetic measurements of $(\text{Rb}_{1-x}\text{Cs}_x)_2\text{Cu}_3\text{SnF}_{12}$ with various x values and the specific-heat measurement of $\text{Cs}_2\text{Cu}_3\text{SnF}_{12}$.

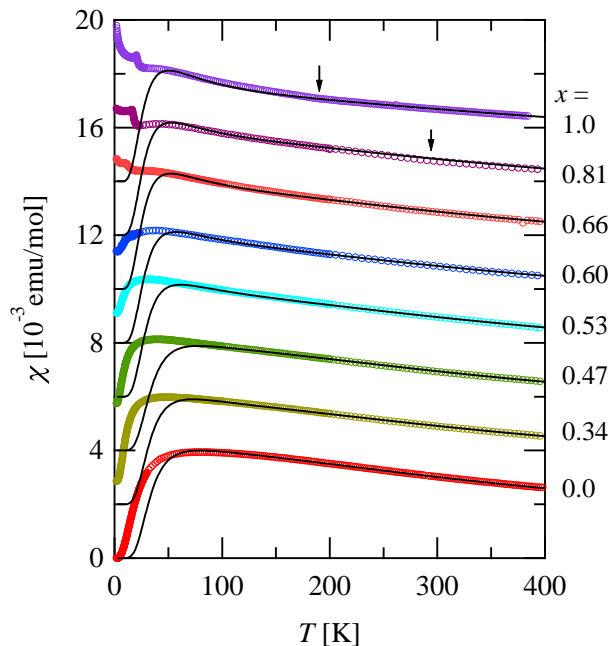


FIG. 2: Temperature dependence of magnetic susceptibility of $(\text{Rb}_{1-x}\text{Cs}_x)_2\text{Cu}_3\text{SnF}_{12}$ measured at $H=1$ T for $H \parallel c$ for various x . The susceptibility data are shifted upward by multiples of 2×10^{-3} emu/mol. The data for $x \leq 0.47$ are corrected for the Curie-Weiss term attributable to impurities. Arrows indicate anomalies associated with structural phase transitions. Solid curves are fits using the theoretical susceptibilities obtained from the exact diagonalization of a 12-site kagome cluster (see text).

The analysis of magnetic susceptibility using exact diagonalization calculations for a 12-site kagome cluster shows that the exchange interactions tend to become more uniform as x increases. It was found that with increasing x , the disordered ground state changes to the ordered state at $x_c \simeq 0.53$, as shown below. The magnitude of the spin gap decreases and approaches zero at x_c , while the ordering temperature T_N decreases as x decreases from 1 and also appears to be zero at x_c . These observations indicate the occurrence of a quantum phase transition at $x_c \simeq 0.53$.

II. EXPERIMENTAL DETAILS

We synthesized $(\text{Rb}_{1-x}\text{Cs}_x)_2\text{Cu}_3\text{SnF}_{12}$ single crystals from a melt comprising a mixture of $\text{Rb}_2\text{Cu}_3\text{SnF}_{12}$ and $\text{Cs}_2\text{Cu}_3\text{SnF}_{12}$ in the ratio of $1-x$ to x . Single crystals of $A_2\text{Cu}_3\text{SnF}_{12}$ ($A = \text{Cs}, \text{Rb}$) were grown by a procedure similar to that reported in previous papers.^{28,29,31,33} The cesium concentration x was determined by inductively coupled plasma mass spectroscopy (ICP-MS) at the Center for Advanced Materials Analysis, Tokyo Institute of Technology. We confirmed that the x-ray powder diffraction pattern obtained using MiniFlexII (Rigaku) changes

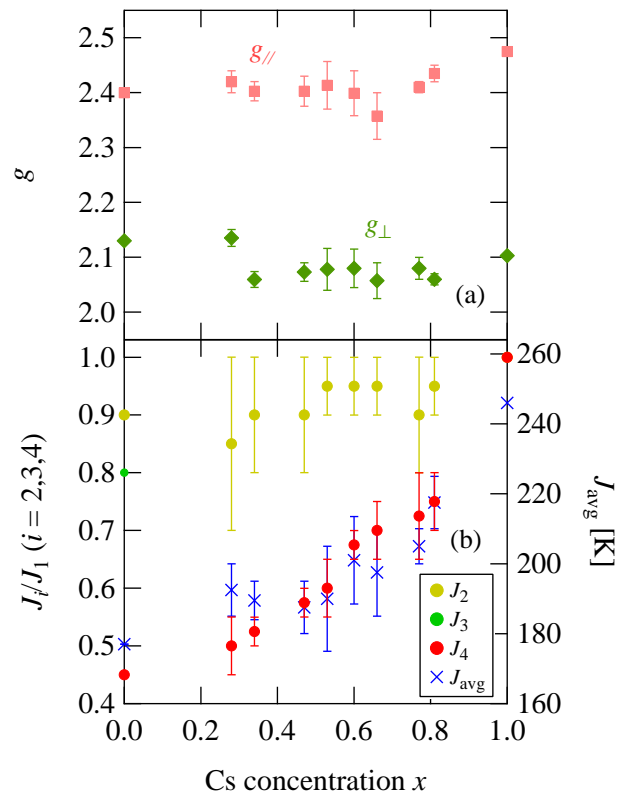


FIG. 3: g factors and exchange parameters as a function of the cesium concentration x in $(\text{Rb}_{1-x}\text{Cs}_x)_2\text{Cu}_3\text{SnF}_{12}$, evaluated from the analyses of magnetic susceptibilities. (a) g_{\parallel} and g_{\perp} for $H \parallel c$ and $H \perp c$, respectively. (b) The individual exchange parameters normalized by J_1 and the average exchange interaction J_{avg} .

systematically with x and that the Bragg peaks are as sharp as those in pure cases with $x=0$ and 1, which indicates high homogeneity of the single crystals. Magnetic susceptibilities were measured under a magnetic field of 1 T in the temperature range 1.8 – 400 K using a superconducting quantum interference device magnetometer (Quantum Design: MPMS XL). Magnetic fields were applied parallel and perpendicular to the c axis. The magnetic susceptibility and magnetization data presented in this paper are corrected for the diamagnetism of core electrons⁴⁴ and the Van Vleck paramagnetism, as described in Ref. 29. The specific heat was measured down to 0.36 K in zero magnetic field using a physical property measurement system (Quantum Design: PPMS) by the relaxation method.

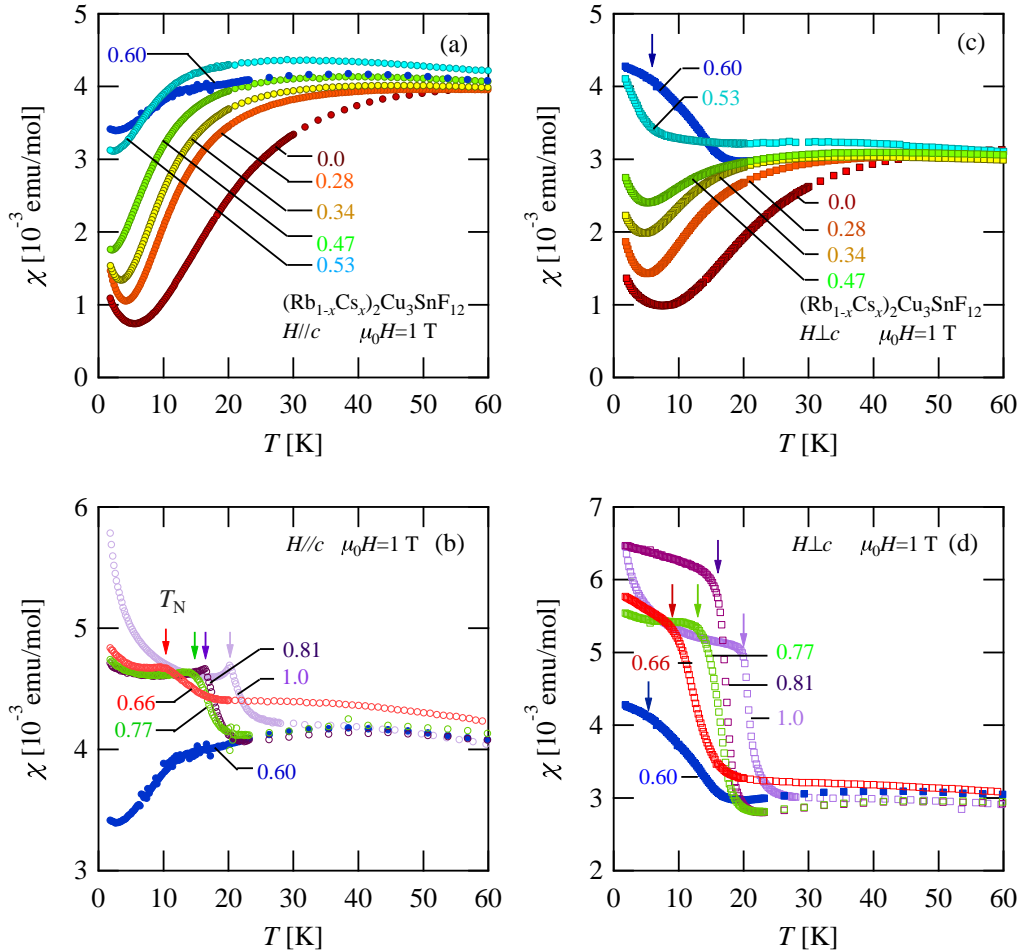


FIG. 4: Measured low-temperature magnetic susceptibility of $(\text{Rb}_{1-x}\text{Cs}_x)_2\text{Cu}_3\text{SnF}_{12}$ for various x measured at $H = 1$ T (a) and (b) for $H \parallel c$ and (c) and (d) for $H \perp c$. (a) and (c) show the data for $0 \leq x \leq 0.60$, and (b) and (d) show the data for $0.60 \leq x \leq 1.0$. Arrows indicate the ordering temperature T_N .

III. RESULTS AND DISCUSSION

A. Exchange parameters

Figure 2 shows the temperature dependence of the magnetic susceptibility χ of $(\text{Rb}_{1-x}\text{Cs}_x)_2\text{Cu}_3\text{SnF}_{12}$ measured at $H = 1$ T for $H \parallel c$ for various x . The data for $x \leq 0.47$ are corrected for the Curie-Weiss term attributable to impurities. With decreasing temperature, the susceptibility for $\text{Rb}_2\text{Cu}_3\text{SnF}_{12}$ ($x=0$) exhibits a rounded maximum at approximately $T_{\text{max}} = 70$ K and decreases to zero, indicating a gapped singlet ground state. As the cesium concentration x is increased, T_{max} decreases and the magnetic susceptibility has a finite value at $T=0$. With further increasing x , a kink anomaly indicating magnetic ordering is observed. Details of the low-temperature susceptibility will be discussed later. For $\text{Cs}_2\text{Cu}_3\text{SnF}_{12}$ ($x=1.0$), the small bend anomaly shown by an arrow, indicating a structural phase transition,

was observed at $T_t = 184$ K, as previously reported.²⁹ For $x=0.81$, the bend anomaly due to the structural phase transition occurs at $T_t = 295$ K. This indicates that T_t increases with decreasing x .

Assuming that the configuration of the nearest-neighbor exchange interaction shown in Fig. 1(c) is common to all $(\text{Rb}_{1-x}\text{Cs}_x)_2\text{Cu}_3\text{SnF}_{12}$ on average, we evaluate the exchange parameters J_i ($i = 1 - 4$) using the exact diagonalization of a 12-site kagome cluster under a periodic boundary condition. For $\text{Cs}_2\text{Cu}_3\text{SnF}_{12}$ ($x=1$) we assume a uniform kagome lattice for simplification as in a previous paper.²⁹ The calculation procedure has been presented in the previous papers.^{28,29} From the fitting to the high-temperature magnetic susceptibility for $T > 200$ K, we evaluate the average exchange interaction J_{avg} . For $\text{Rb}_2\text{Cu}_3\text{SnF}_{12}$ ($x=0$), we confirmed that the magnetic susceptibility is satisfactorily reproduced using $J_1/k_B = 216$ K, $J_2 = 0.95J_1$, $J_3 = 0.85J_1$ and $J_4 = 0.55J_1$ obtained from the analysis of the dispersion relations.³² Thus, individual values of J_i/J_1 can be estimated from

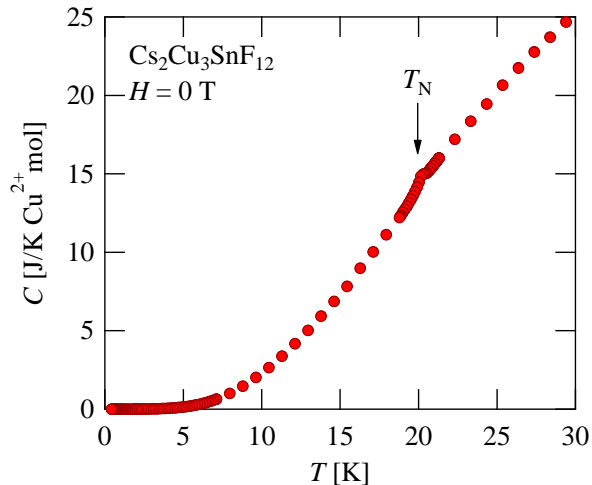


FIG. 5: Specific heat of $\text{Cs}_2\text{Cu}_3\text{SnF}_{12}$ as a function of temperature measured at zero magnetic field. The arrow indicates the ordering temperature T_N .

the fitting to the low-temperature magnetic susceptibility for $T < 200$ K. For the intermediate compounds, we found that the calculated susceptibility is only slightly sensitive to J_3 for $0.5 \leq J_3/J_1 \leq 1.0$, hence we estimated only J_2/J_1 and J_4/J_1 . Meanwhile, J_3/J_1 could not be determined uniquely. The solid lines in Fig. 2 are fits with the parameters shown in Fig. 3. We also performed the same analysis on the susceptibility data for $H \perp c$. The exchange parameters shown in Fig. 3 are obtained by fitting for both $H \parallel c$ and $H \perp c$. In the present analysis, we neglect the DM interaction because its effect on the susceptibility for $T > 60$ K is small.³¹

As shown in Fig. 2, the calculated susceptibilities accurately reproduce the experimental susceptibilities for $T > 60$ K in all $(\text{Rb}_{1-x}\text{Cs}_x)_2\text{Cu}_3\text{SnF}_{12}$, while for $T < 60$ K, the calculated susceptibility decreases more rapidly than the experimental susceptibility. This should be due to the finite-size effect. Figure 3 summarizes the x dependence of the magnetic parameters for $(\text{Rb}_{1-x}\text{Cs}_x)_2\text{Cu}_3\text{SnF}_{12}$ determined from the susceptibility analyses using the exact diagonalization calculations. g_{\parallel} and g_{\perp} denote the g factors for $H \parallel c$ and $H \perp c$, respectively. We incorporate the g factor into the fitting parameters because it is difficult to determine the g factor by the usual electron paramagnetic resonance because of the extremely large line-width arising from the large DM interaction. The g factors obtained with the present analysis are independent of x . The magnitude of the g factors, i.e., $g_{\parallel} = 2.4 - 2.5$ and $g_{\perp} = 2.1$, are consistent with those for K_2CuF_4 and Rb_2CuF_4 .⁴⁵ As shown Fig. 3(b), the average of the four sorts of exchange interactions J_{avg} increases monotonically as $x \rightarrow 1$. J_4/J_1 increases rapidly with increasing x . The calculated susceptibility is insensitive to J_3 for $0.5 \leq J_3/J_1 \leq 1.0$, as mentioned above. Because the smallest J_4/J_1 increases

with increasing x , we infer that all the exchange interactions approach a uniform value for $x \rightarrow 1$.

B. Ground-state phase diagram

Figure 4 shows the low-temperature magnetic susceptibility of $(\text{Rb}_{1-x}\text{Cs}_x)_2\text{Cu}_3\text{SnF}_{12}$ measured at $H = 1$ T for $H \parallel c$ and $H \perp c$ for various x . For $x \leq 0.47$, the susceptibility exhibits a small upturn below 7 K, which should be due mainly to the impurity phase. With increasing x , the temperature T_{max} giving the rounded maximum of susceptibility decreases. This behavior of susceptibility is considered to be related to the fact that the exchange interactions become uniform with increasing x . The low-temperature susceptibility for $x \leq 0.47$ corrected for the upturn below 7 K shows exponential temperature dependence indicative of the presence of an excitation gap. For $x \leq 0.53$, no anomaly indicative of magnetic ordering is observed. This shows that the ground state is disordered for $x \leq 0.53$. On the other hand, the susceptibility for $x \geq 0.60$ exhibits kink or bend anomalies, which are suggestive of magnetic ordering. For $x = 0.60$, we assigned the temperature at which a small bend anomaly appears for $H \perp c$ as the ordering temperature T_N .

Figure 5 shows the temperature dependence of the specific heat for $\text{Cs}_2\text{Cu}_3\text{SnF}_{12}$. A tiny cusp anomaly owing to magnetic ordering is observed at $T_N = 20.0$ K. This ordering temperature coincides with that assigned from the anomaly in the susceptibility. The very small anomaly in the specific heat around T_N indicates that little entropy remains for magnetic ordering because of the well-developed short-range spin correlation caused by the large exchange interaction of $J/k_B \simeq 240$ K and good two-dimensionality. For $x \neq 1$, the specific heat anomaly is so small that it is difficult to detect the magnetic ordering.

The transition data obtained from the low-temperature susceptibilities are summarized in Fig. 6. With decreasing x , the ordering temperature T_N decreases, and T_N reaches zero at $x_c \simeq 0.53$.

We analyze the low-temperature susceptibility for $x \leq 0.47$ using the following formula:

$$\chi(T) = \frac{C}{T - \Theta} + A \exp\left(-\frac{\Delta}{k_B T}\right) + \chi_0, \quad (1)$$

where the first term is the Curie-Weiss term, the second term represents the low-temperature susceptibility for two-dimensional systems with an excitation gap Δ ,^{46,47} and the last constant term arises from the finite susceptibility component in the ground state.

Here we estimate x dependence of χ_0 from the magnetization curves of $(\text{Rb}_{1-x}\text{Cs}_x)_2\text{Cu}_3\text{SnF}_{12}$ ($0 \leq x \leq 0.47$) for $H \parallel c$ at 1.8 K shown in Fig. 7. The magnetization data have been corrected for impurity contributions which are assumed to follow the Brillouin function. The impurity concentration were evaluated to be between 0.4 % and 0.7 %. For $x = 0$, the highest applied field of 7 T is

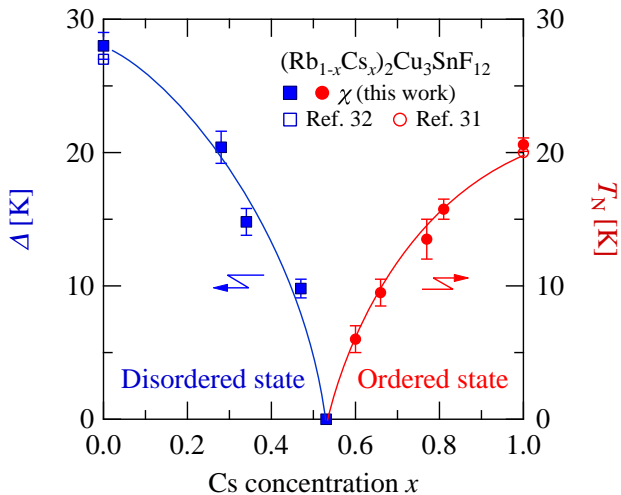


FIG. 6: Phase diagram of the spin gap Δ and Néel temperature T_N for $(\text{Rb}_{1-x}\text{Cs}_x)_2\text{Cu}_3\text{SnF}_{12}$, determined via magnetic measurements with $H \parallel c$. Δ is estimated by fitting the susceptibility data using Eq. (1). Results obtained in other measurements^{31,32} are also shown for comparison.

smaller than the critical value $H_c = 13$ T, where the excitation gap closes.^{28,29} The magnetization slope below 2 T is very small but finite, from which χ_0 is estimated to be $\chi_0 \simeq 1 \times 10^{-4}$ emu/mol. The residual susceptibility χ_0 for $H \perp c$ is estimated as $\chi_0 \simeq 4 \times 10^{-4}$ emu/mol, which is four times larger than that for $H \parallel c$. The finite χ_0 is attributed to the small transverse component D^\perp of the \mathbf{D} vector for the DM interaction.⁴⁸ Figure 8 summarizes the residual susceptibility χ_0 for $x \leq 0.47$ estimated from the magnetization slope. The residual susceptibility χ_0 is finite for $H \parallel c$ even in the disordered ground state and exhibits a rapid increase with increasing x . For $x = 0.47$, magnetization increases rapidly up to $H_c \sim 6.2$ T and increases linearly with increasing magnetic field. The magnitude of the gap ($\simeq 9.8$ K) for $x = 0.47$ is consistent with that obtained from the low-temperature susceptibility using Eq. (1), as shown below.

Fitting Eq. (1) to the low-temperature susceptibility of $\text{Rb}_2\text{Cu}_3\text{SnF}_{12}$ for $H \parallel c$ with $\chi_0 \simeq 1 \times 10^{-4}$ emu/mol, we obtain $\Delta/k_B = 28$ K, which is consistent with $\Delta/k_B = 27$ K observed by neutron inelastic scattering.^{32,33} This guarantees the validity of the present analysis. The x dependence of the excitation gap Δ obtained by fitting Eq. (1) with χ_0 shown in Fig. 8 is shown in Fig. 6. With increasing x , Δ diminishes and vanishes at $x_c \simeq 0.53$. Because both the excitation gap Δ and the ordering temperature T_N become zero at $x_c \simeq 0.53$, we can deduce that a quantum phase transition from the disordered state to the ordered state takes place at $x = x_c$. Therefore, $x_c \simeq 0.53$ should be the quantum critical point.

The ground states for the quantum triangular lattice and kagome lattice antiferromagnets with bond randomness and site dilution have been discussed theoret-

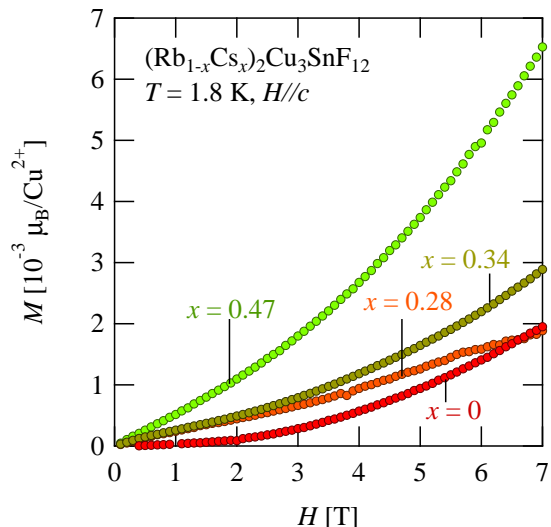


FIG. 7: Magnetization curves of $(\text{Rb}_{1-x}\text{Cs}_x)_2\text{Cu}_3\text{SnF}_{12}$ measured for $H \parallel c$ at $T = 1.8$ K. The data were corrected for impurity contributions represented by the Brillouin function.

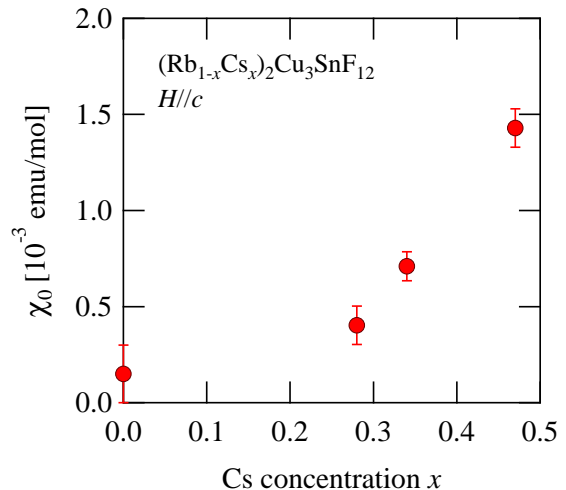


FIG. 8: Residual susceptibility χ_0 for $H \parallel c$ in the disordered ground state for $0 \leq x \leq 0.47$.

ically, and the valence-bond-glass (VBG) phase was argued to be the ground state.^{49–52} The VBG phase has finite susceptibility but no long-range ordering. The VBG phase is similar to the Bose glass phase, which emerges in an interacting boson system with random potential^{53,54} and/or in a disordered dimer magnet in a magnetic field.^{55–58} The low-temperature magnetic properties characteristic of the VBG have actually been observed in the spatially anisotropic triangular-lattice antiferromagnet $\text{Cs}_2\text{Cu}(\text{Br}_{1-x}\text{Cl}_x)_4$.⁵⁹ Because the magnetic susceptibility of $(\text{Rb}_{1-x}\text{Cs}_x)_2\text{Cu}_3\text{SnF}_{12}$ in the ground state is finite for $0 < x \leq 0.47$, the ground state appears

to be gapless. Hence the gap Δ shown in Fig. 6 should be the pseudogap. Because the ground state properties for $0 < x \leq 0.47$ are consistent with those for the VBG, we infer that the ground state can be described as the VBG and that the phase transition at $x_c \simeq 0.53$ corresponds to the transition from the VBG state to the ordered state with the $q = 0$ structure. Microscopic measurements are necessary to clarify the nature of the disordered ground state in $(\text{Rb}_{1-x}\text{Cs}_x)_2\text{Cu}_3\text{SnF}_{12}$.

Note that the temperature dependence of the magnetic susceptibility of $(\text{Rb}_{1-x}\text{Cs}_x)_2\text{Cu}_3\text{SnF}_{12}$ for $0 < x \leq 0.47$ is similar to that of the $S = 1/2$ kagome-lattice antiferromagnet herbertsmithite, $\text{ZnCu}_3(\text{OH})_6\text{Cl}_2$, extracted from the Knight shift of NMR spectra.^{60,61} This will give insight into the ground state of herbertsmithite. In an actual sample of herbertsmithite, Cu^{2+} partially substitutes for Zn^{2+} .²⁶ Cu^{2+} in an octahedral environment is Jahn-Teller active. Consequently, the substituted Cu^{2+} pushes and pulls the surrounding oxygen ions, which leads to disorder in the oxygen position. Because the oxygen mediates the superexchange interaction in the kagome layer and the superexchange interaction is sensitive to the bond angle of $\text{Cu}^{2+} - \text{O}^{2-} - \text{Cu}^{2+}$, the exchange interaction in the kagome layer is considered to be nonuniform, as in $(\text{Rb}_{1-x}\text{Cs}_x)_2\text{Cu}_3\text{SnF}_{12}$. Therefore, it is plausible that the ground state of the actual sample of herbertsmithite is similar to that in the disordered state of $(\text{Rb}_{1-x}\text{Cs}_x)_2\text{Cu}_3\text{SnF}_{12}$.

IV. CONCLUSION

We have systematically investigated the variation in the exchange interactions and the magnetic ground states

in the spatially anisotropic kagome-lattice antiferromagnet $(\text{Rb}_{1-x}\text{Cs}_x)_2\text{Cu}_3\text{SnF}_{12}$ by magnetic susceptibility measurements. It was found that the four sorts of nearest-neighbor exchange interactions tend to become more uniform with increasing cesium concentration x . We have found that a quantum phase transition from the disordered state to the ordered state occurs at $x_c \simeq 0.53$. The disordered state for $x < x_c$ has finite magnetic susceptibility and a pseudogap Δ , which decreases with increasing x and vanishes at x_c . The disordered state is concluded to be the valence-bond-glass state.

ACKNOWLEDGMENTS

We are indebted to S. Hirata for his technical advice on the exact diagonalization. We express our profound gratitude to Y. Ohtsuka for assistance with ICP-MS analysis. K. K. acknowledges the financial support from the Center of Excellence Program by MEXT, Japan through the ‘‘Nanoscience and Quantum Physics’’ Project of the Tokyo Institute of Technology. This work was supported by Grant-in-Aid for Scientific Research (A) (Grants No. 23244072 and No. 26247058) and Grant-in-Aid for Young Scientists (B) (Grant No. 26800181) from the Japan Society for the Promotion of Science.

* Electronic address: katayama.k.ad@m.titech.ac.jp

† Electronic address: kurita.n.aa@m.titech.ac.jp

‡ Electronic address: tanaka@lee.phys.titech.ac.jp

¹ L. Balents, *Nature (London)* **464**, 199 (2010).

² A. Chubukov, *Phys. Rev. Lett.* **69**, 832 (1992).

³ S. Sachdev, *Phys. Rev. B* **45**, 12377 (1992).

⁴ M. J. Lawler, L. Fritz, Y. B. Kim, and S. Sachdev, *Phys. Rev. Lett.* **100**, 187201 (2008).

⁵ R. R. P. Singh and D. A. Huse, *Phys. Rev. B* **77**, 144415 (2008).

⁶ E. S. Sørensen, M. J. Lawler, and Y. B. Kim, *Phys. Rev. B* **79**, 174403 (2009).

⁷ G. Evenbly and G. Vidal, *Phys. Rev. Lett.* **104**, 187203 (2010).

⁸ K. Hwang, Y. B. Kim, J. Yu, and K. Park: *Phys. Rev. B* **84**, 205133 (2011).

⁹ M. B. Hastings, *Phys. Rev. B* **63**, 014413 (2000).

¹⁰ F. Wang and A. Vishwanath, *Phys. Rev. B* **74**, 174423 (2006).

¹¹ M. Hermele, Y. Ran, P. A. Lee, and X.-G. Wen, *Phys. Rev. B* **77**, 224413 (2008).

¹² S. Yan, D. A. Huse, and S. R. White, *Science* **332**, 1173

(2011).

¹³ Ch. Waldtmann, H. U. Everts, B. Bernu, C. Lhuillier, P. Sindzingre, P. Lecheminant, and L. Pierre, *Eur. Phys. J. B* **2**, 501 (1998).

¹⁴ H. Nakano and T. Sakai, *J. Phys. Soc. Jpn.* **80**, 053704 (2011).

¹⁵ S. Depenbrock, I. P. McCulloch, and U. Schollwöck, *Phys. Rev. Lett.* **109**, 067201 (2012).

¹⁶ S. Nishimoto, N. Shibata, and C. Hotta, *Nat. Commun.* **4**, 2287 (2013).

¹⁷ Z. Hiroi, M. Hanawa, N. Kobayashi, M. Nohara, H. Takagi, Y. Kato, and M. Takigawa, *J. Phys. Soc. Jpn.* **70**, 3377 (2001).

¹⁸ H. Yoshida, J. Yamaura, M. Isobe, Y. Okamoto, G. J. Nilsen and Z. Hiroi, *Nat. Commun.* **3**, 860 (2012).

¹⁹ M. Yoshida, Y. Okamoto, M. Takigawa, and Z. Hiroi, *J. Phys. Soc. Jpn.* **82**, 013702 (2013).

²⁰ Y. Okamoto, H. Yoshida, and Z. Hiroi, *J. Phys. Soc. Jpn.* **78**, 033701 (2009).

²¹ M. P. Shores, E. A. Nytko, B. M. Bartlett, and D. G. Nocera, *J. Am. Chem. Soc.* **127**, 13462 (2005).

²² P. Mendels, F. Bert, M. A. de Vries, A. Olariu, A. Harrison,

- F. Duc, J. C. Trombe, J. S. Lord, A. Amato, and C. Baines, *Phys. Rev. Lett.* **98**, 077204 (2007).
- ²³ J. S. Helton, K. Matan, M. P. Shores, E. A. Nytko, B. M. Bartlett, Y. Yoshida, Y. Takano, A. Suslov, Y. Qiu, J. -H. Chung, D. G. Nocera, and Y. S. Lee, *Phys. Rev. Lett.* **98**, 107204 (2007).
- ²⁴ M. Müller and B. G. Müller, *Z. Anorg. Allg. Chem.* **621**, 993 (1995).
- ²⁵ O. Janson, J. Richter, P. Sindzingre, and H. Rosner, *Phys. Rev. B* **82**, 104434 (2010).
- ²⁶ F. Bert, S. Nakamae, F. Ladieu, D. L'Hôte, P. Bonville, F. Duc, J.-C. Trombe, and P. Mendels, *Phys. Rev. B* **76**, 132411 (2007).
- ²⁷ S. A. Reisinger, C. C. Tang, S. P. Thompson, F. D. Morrison, and P. Lightfoot, *Chem. Mater.* **23**, 4234 (2011).
- ²⁸ K. Morita, M. Yano, T. Ono, H. Tanaka, K. Fujii, H. Uekusa, Y. Narumi, and K. Kindo, *J. Phys. Soc. Jpn.* **77**, 043707 (2008).
- ²⁹ T. Ono, K. Morita, M. Yano, H. Tanaka, K. Fujii, H. Uekusa, Y. Narumi, and K. Kindo, *Phys. Rev. B* **79**, 174407 (2009).
- ³⁰ L. J. Downie, C. Black, E. I. Ardashnikova, C. C. Tang, A. N. Vasiliev, A. N. Golovanov, P. S. Berdonosov, V. A. Dolgikh, and P. Lightfoot, *CrystEngComm.* **16**, 7419 (2014).
- ³¹ T. Ono, K. Matan, Y. Nambu, T. J. Sato, K. Katayama, S. Hirata, and H. Tanaka, *J. Phys. Soc. Jpn.* **83**, 043701 (2014).
- ³² K. Matan, T. Ono, Y. Fukumoto, T. J. Sato, J. Yamaura, M. Yano, K. Morita, and H. Tanaka, *Nat. Phys.* **6**, 865 (2010).
- ³³ K. Matan, Y. Nambu, Y. Zhao, T. J. Sato, Y. Fukumoto, T. Ono, H. Tanaka, C. Broholm, A. Podlesnyak, and G. Ehlers, *Phys. Rev. B* **89**, 024414 (2014).
- ³⁴ M. S. Grbić, S. Krämer, C. Berthier, F. Trouselet, O. Cépas, H. Tanaka, and M. Horvatić, *Phys. Rev. Lett.* **110**, 247203 (2013).
- ³⁵ B. J. Yang and Y. B. Kim, *Phys. Rev. B* **79**, 224417 (2009).
- ³⁶ E. Khatami, R. R. P. Singh, and M. Rigol, *Phys. Rev. B* **84**, 224411 (2011).
- ³⁷ O. Cépas, C. M. Fong, P. W. Leung, and C. Lhuillier, *Phys. Rev. B* **78**, 140405(R) (2008).
- ³⁸ J. des Cloizeaux and J. J. Pearson, *Phys. Rev.* **128**, 2131 (1962).
- ³⁹ Y. Endoh, G. Shirane, R. Birgeneau, P. Richards, and S. Holt, *Phys. Rev. Lett.* **32**, 170 (1974).
- ⁴⁰ J. Igarashi, *Phys. Rev. B* **46**, 10763 (1992).
- ⁴¹ R. R. P. Singh, and M. P. Gelfand, *Phys. Rev. B* **52**, R15695 (1995).
- ⁴² H. M. Rønnow, D. F. McMorrow, R. Coldea, A. Harrison, I. D. Youngson, T. G. Perring, G. Aeppli, O. Syljuåsen, K. Lefmann, and C. Rischel, *Phys. Rev. Lett.* **87**, 037202 (2001).
- ⁴³ K. Hwang, K. Park, and Y. B. Kim, *Phys. Rev. B* **86**, 214407 (2012).
- ⁴⁴ P. W. Selwood, *Magnetochemistry* (Wiley-Interscience, New York, 1956) 2nd ed., Chap. 2, p. 78.
- ⁴⁵ S. Sasaki, N. Narita, and I. Yamada, *J. Phys. Soc. Jpn.* **64**, 2701 (1995).
- ⁴⁶ M. Troyer, H. Tsunetsugu, and D. Würtz, *Phys. Rev. B* **50**, 13515 (1994).
- ⁴⁷ M. B. Stone, I. Zaliznyak, D. H. Reich, and C. Broholm, *Phys. Rev. B* **64**, 144405 (2001).
- ⁴⁸ K. Sasao, N. Kunisada, and Y. Fukumoto, unpublished result. K. Sasao, N. Kunisada, and Y. Fukumoto, Meeting Abst. Phys. Soc. Jpn. **65(2-3)**, 442 (2010). (in Japanese)
- ⁴⁹ M. Tarzia and G. Biroli, *Europhys. Lett.* **82**, 67008 (2008).
- ⁵⁰ R. R. P. Singh, *Phys. Rev. Lett.* **104**, 177203 (2010).
- ⁵¹ K. Watanabe, H. Kawamura, H. Nakano, and T. Sakai, *J. Phys. Soc. Jpn.* **83**, 034714 (2014).
- ⁵² H. Kawamura, K. Watanabe, and T. Shimokawa, *J. Phys. Soc. Jpn.* **83**, 103704 (2014).
- ⁵³ T. Giamarchi and H. J. Schulz, *Phys. Rev. B* **37**, 325 (1988).
- ⁵⁴ M. P. A. Fisher, P. B. Weichman, G. Grinstein, and D. S. Fisher, *Phys. Rev. B* **40**, 546 (1989).
- ⁵⁵ A. Oosawa and H. Tanaka, *Phys. Rev. B* **65**, 184437 (2002).
- ⁵⁶ Y. Shindo and H. Tanaka, *J. Phys. Soc. Jpn.* **73**, 2642 (2004).
- ⁵⁷ F. Yamada, H. Tanaka, T. Ono, and H. Nojiri, *Phys. Rev. B* **83**, 020409(R) (2011).
- ⁵⁸ A. Zheludev and T. Roscilde, *C. R. Phys.* **14**, 740 (2013).
- ⁵⁹ T. Ono, H. Tanaka, T. Nakagomi, O. Kolomiyets, H. Mitamura, F. Ishikawa, T. Goto, K. Nakajima, A. Oosawa, Y. Koike, K. Kakurai, J. Klenke, P. Smeibidle, M. Meisner, and H. A. Katori, *J. Phys. Soc. Jpn.* **74** (Suppl.), 135 (2005).
- ⁶⁰ T. Imai, E. A. Nytko, B. M. Bartlett, M. P. Shores, and D. G. Nocera, *Phys. Rev. Lett.* **100**, 077203 (2008).
- ⁶¹ A. Olariu, P. Mendels, F. Bert, F. Duc, J. C. Trombe, M. A. de Vries, and A. Harrison, *Phys. Rev. Lett.* **100**, 087202 (2008).